

## A New Method for the 2D DOA Estimation of Coherently Distributed Sources

Liang Zhou

University of Electronic Science and Technology of China, No.2006, Xiyuan Ave, West Hi-Tech Zone, Chengdu, Sichuan, P. R. China, 611731, China

Tel.: +86 02861831106

E-mail: zlzl@uestc.edu.cn

*Received: 24 February 2014 /Accepted: 28 March 2014 /Published: 31 March 2014*

**Abstract:** The purpose of this paper is to develop a new technique for estimating the two-dimensional (2D) direction-of-arrivals (DOAs) of coherently distributed (CD) sources, which can estimate effectively the central azimuth and central elevation of CD sources at the cost of less computational cost. Using the special L-shape array, a new approach for parametric estimation of CD sources is proposed. The proposed method is based on two rotational invariance relations under small angular approximation, and estimates two rotational matrices which depict the relations, using propagator technique. And then the central DOA estimations are obtained by utilizing the primary diagonal elements of two rotational matrices. Simulation results indicate that the proposed method can exhibit a good performance under small angular spread and be applied to the multisource scenario where different sources may have different angular distribution shapes. Without any peak-finding search and the eigendecomposition of the high-dimensional sample covariance matrix, the proposed method has significantly reduced the computational cost compared with the existing methods, and thus is beneficial to real-time processing and engineering realization. In addition, our approach is also a robust estimator which does not depend on the angular distribution shape of CD sources. *Copyright © 2014 IFSA Publishing, S. L.*

**Keywords:** Coherently distributed sources, 2D DOA estimation, L-shape array, Propagator.

### 1. Introduction

Direction of arrival (DOA) estimation is a major research domain in array signal processing. Most of DOA estimation methods have been designed for sources that are modeled as points in space. However, in many applications such as wireless communications, radar and sonar and so on, aim signals have sometimes spatially distributed property. The performance of the methods based on point sources assumption will degenerate notably under distributed signals. Therefore, the DOA estimation of distributed sources becomes a problem for special research. In general, distributed sources

can be modeled as coherently distributed (CD) sources and incoherently distributed (ID) sources [1, 2]. When the signal components from a source at different angles are the delayed and scaled replicas of the same signal, the source is called CD sources. When the signal rays arriving from different directions are uncorrelated, the source is called ID sources.

For CD sources, several classical techniques for DOA estimation have been proposed in the past few decades. The maximum likelihood (ML) estimator is derived in [3] and [4]. Modifications and generalizations of the classical MUSIC algorithm have given rise to the algorithms VEC-MUSIC [5],

DSPE [6], and generalized MUSIC [7]. ESPRIT is extended for distributed sources parameter estimation by using two closely-spaced ULAs [8] or generalized eigendecomposition [9-11]. Min-minimum eigenvalue method and max-maximum eigenvalue method are introduced in [12]. A generalized beamforming estimator is used to estimate the parameters of CD sources in [13]. Sparse signal representation (SRR) is proposed in [14].

All these techniques above aim at one-dimensional (1D) CD sources. However, in three-dimensional practical environment, the impinging signal is not generally in the same plane with the receiving array, which should be modeled as two-dimensional (2D) distributed source. Consequently, it is more valuable to research the DOA estimation of 2D CD sources. For 2D CD sources, the conventional methods will involve a great computational burden owing to multi-dimensional optimization. Therefore, it is always a concerned focus in this domain to find some low-complexity methods.

In the literatures [15, 16, 10, 11], several DOA estimation techniques for 2D CD sources are presented by using L-linear array or uniform circular array (UCA). It is common characteristic that they transform a four-dimensional parameter optimization problem into two 2D parameter optimization problems, so the computational complexity is decreased to some extent. Based on two parallel UCAs and the relation between the signal subspace and steering vector, a sequential one-dimensional searching (SOS) algorithm is proposed for the central DOA estimation of 2D CD sources in [17]. Its main idea is that the preliminary estimate of the central elevation is firstly given by the TLS-ESPRIT method, and then the central azimuth and elevation are estimated by sequential 1D searching. SOS significantly reduces computational cost, due to using only 1D search.

However, the above methods still involve intensive computation owing to peak-finding search. Moreover, most of them are not robust to angular distribution shape. In [18], an algorithm called the quadric rotational invariance property (QRIP) has been presented for estimating the central DOAs of 2D CD sources. Without any peak-finding search, QRIP can realize the decoupled estimation of the central azimuth and elevation. In addition, a low-complexity 2D DOA estimator method which is for CD sources is proposed in [19]. It does not require peak-finding search and depend on angular distribution shape.

In this paper, we have proposed a new algorithm for estimating the central DOAs of 2D CD sources. The proposed method firstly uses a propagator method [20] to estimate two rotational matrices which denote two approximate rotational invariance relationships. And then the central DOAs are computed through the primary diagonal elements of two rotational matrices. Our approach doesn't

involve any peak-finding search and the eigendecomposition of the high-dimensional sample covariance matrix in conventional methods, which has significantly reduced computational cost. Moreover, it is robust to the angular distribution shape. Simulation results demonstrate the effectiveness of the proposed method.

## 2. Date Model

Consider the L-shape array geometry as depicted in Fig. 1. It consists of two ULAs X and Y. Each array contains M sensor elements, and the distance of adjacent sensors in each ULA is d. Assuming that q uncorrelated narrowband signals impinge on the array. In addition, it is assumed that the noise in each sensor is the additive white Gaussian noise, and noise is irrelevant to signal.

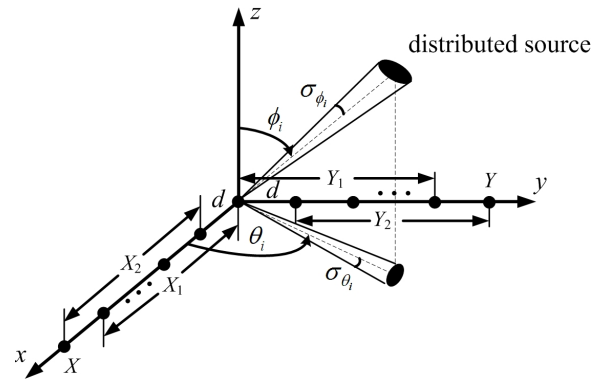


Fig. 1. L-shape array geometry.

### 2.1. Classical Data Model

For 2D distributed sources, the outputs of the arrays X and Y can be expressed as:

$$\begin{cases} \mathbf{x}(t) = \sum_{i=1}^q \iint \mathbf{a}_X(\theta, \phi) s_i(\theta, \phi; t) d\theta d\phi + \mathbf{n}_X(t) \\ \mathbf{y}(t) = \sum_{i=1}^q \iint \mathbf{a}_Y(\theta, \phi) s_i(\theta, \phi; t) d\theta d\phi + \mathbf{n}_Y(t) \end{cases} \quad (1)$$

where  $\mathbf{x}(t)$  and  $\mathbf{y}(t)$  are the  $M \times 1$  received data vector.  $\mathbf{n}_X(t)$  and  $\mathbf{n}_Y(t)$  are the  $M \times 1$  noise vector.  $\mathbf{a}_X(\theta, \phi) = [1, e^{j\eta \sin\phi \cos\theta}, \dots, e^{j\eta(M-1)\sin\phi \cos\theta}]^T$  is the  $M \times 1$  steering vector for a point source for X array ( $\eta = 2\pi d / \lambda$ , and  $\lambda$  is the wavelength of the impinging signal).

$\mathbf{a}_Y(\theta, \phi) = [1, e^{j\eta \sin\phi \sin\theta}, \dots, e^{j\eta(M-1)\sin\phi \sin\theta}]^T$  is the  $M \times 1$  steering vector for a point source for Y array.  $s_i(\theta, \phi; t)$  is the angular signal density function of the  $i^{\text{th}}$  source, and is parameterized by the vector  $\mu_i = (\theta_i, \sigma_{\theta_i}, \phi_i, \sigma_{\phi_i})$  denoting the central azimuth,

azimuth angular spread, central elevation and elevation angular spread, respectively. Notice that the integrating ranges in (1) have been omitted for the simplicity.

For CD sources,  $s_i(\theta, \phi; t)$  can be written as:

$$s_i(\theta, \phi; t) = s_i(t)g_i(\theta, \phi; \mu_i), \quad (2)$$

where  $s_i(t)$  is the random signal, and  $g_i(\theta, \phi; \mu_i)$  is the deterministic angular distribution function of the  $i^{\text{th}}$  source, and is parameterized by the vector  $\mu_i = (\theta_i, \sigma_{\theta_i}, \phi_i, \sigma_{\phi_i})$ .

Define the generalized steering vectors (GSVs) of the arrays  $X$  and  $Y$  as follows:

$$\mathbf{b}_X(\mu_i) = \iint \mathbf{a}_X(\theta, \phi)g_i(\theta, \phi; \mu_i)d\theta d\phi, \quad (3)$$

$$\mathbf{b}_Y(\mu_i) = \iint \mathbf{a}_Y(\theta, \phi)g_i(\theta, \phi; \mu_i)d\theta d\phi, \quad (4)$$

Let  $\mathbf{s}(t) = [s_1(t), s_2(t), \dots, s_q(t)]^T$ , (1) can be rewritten in vector form:

$$\begin{cases} \mathbf{x}(t) = \mathbf{B}_X \mathbf{s}(t) + \mathbf{n}_X(t) \\ \mathbf{y}(t) = \mathbf{B}_Y \mathbf{s}(t) + \mathbf{n}_Y(t) \end{cases}, \quad (5)$$

where

$$\mathbf{B}_X = [\mathbf{b}_X(\mu_1), \mathbf{b}_X(\mu_2), \dots, \mathbf{b}_X(\mu_q)], \quad (6)$$

$$\mathbf{B}_Y = [\mathbf{b}_Y(\mu_1), \mathbf{b}_Y(\mu_2), \dots, \mathbf{b}_Y(\mu_q)], \quad (7)$$

Divide  $X$  into two shifted subarrays  $X_1$  and  $X_2$  as depicted in Fig. 1, and the GSVs of  $X_1$  and  $X_2$  can be, respectively, defined as:

$$\mathbf{b}_{X_1}(\mu_i) = \iint \mathbf{D}\mathbf{a}_X(\theta, \phi)g_i(\theta, \phi; \mu_i)d\theta d\phi, \quad (8)$$

$$\mathbf{b}_{X_2}(\mu_i) = \iint \mathbf{D}\mathbf{a}_X(\theta, \phi)e^{j\eta \sin \phi \cos \theta} g_i(\theta, \phi; \mu_i)d\theta d\phi, \quad (9)$$

where  $\mathbf{D} = [\mathbf{I}_{(M-1) \times (M-1)} \mid \mathbf{0}_{(M-1) \times 1}]$ .

Similarly, divide  $Y$  into two shifted subarrays  $Y_1$  and  $Y_2$  as depicted in Fig. 1, and the GSVs of  $Y_1$  and  $Y_2$  are, respectively, defined as:

$$\mathbf{b}_{Y_1}(\mu_i) = \iint \mathbf{D}\mathbf{a}_Y(\theta, \phi)g_i(\theta, \phi; \mu_i)d\theta d\phi, \quad (10)$$

$$\mathbf{b}_{Y_2}(\mu_i) = \iint \mathbf{D}\mathbf{a}_Y(\theta, \phi)e^{j\eta \sin \phi \sin \theta} g_i(\theta, \phi; \mu_i)d\theta d\phi, \quad (11)$$

## 2.2. Taylor Approximation Model

For arbitrary  $\theta$  and  $\phi$ , we define  $\theta = \theta_i + \tilde{\theta}$  and  $\phi = \phi_i + \tilde{\phi}$ . Where  $\tilde{\theta}$ ,  $\tilde{\phi}$  are the small deviations

between  $\theta$ ,  $\phi$  and the nominal DOAs  $\theta_i$ ,  $\phi_i$ . Under small angular extension, by one-order Taylor approximation to the  $k^{\text{th}}$  element of  $\mathbf{a}_X(\theta, \phi)$  around  $(\theta, \phi) = (\theta_i, \phi_i)$ , we have:

$$\begin{aligned} [\mathbf{a}_X(\theta, \phi)]_k &= e^{j\eta(k-1)\sin \phi \cos \theta} = e^{j\eta(k-1)\sin(\phi_i + \tilde{\phi})\cos(\theta_i + \tilde{\theta})} \\ &\approx e^{j\eta(k-1)(\sin \phi_i + \tilde{\phi} \cos \phi_i)(\cos \theta_i - \tilde{\theta} \sin \theta_i)} \\ &= e^{j\eta(k-1)\sin \phi_i \cos \theta_i} e^{j\eta(k-1)(\tilde{\phi} \cos \phi_i \cos \theta_i - \tilde{\theta} \sin \phi_i \sin \theta_i)} \end{aligned} \quad (12)$$

In (12), we use the approximation that  $\tilde{\theta}\tilde{\phi} \approx 0$  for small values of  $\tilde{\theta}$  and  $\tilde{\phi}$ .

Substitute (12) into (8), the  $k^{\text{th}}$  element of  $\mathbf{b}_{X_1}(\mu_i)$  can approximately be written as:

$$[\mathbf{b}_{X_1}(\mu_i)]_k \approx e^{j\eta(k-1)\sin \phi_i \cos \theta_i} [\mathbf{h}(\mu_i)]_k, \quad (13)$$

where

$$\begin{aligned} [\mathbf{h}(\mu_i)]_k &= \iint e^{j\eta(k-1)(\tilde{\phi} \cos \phi_i \cos \theta_i - \tilde{\theta} \sin \phi_i \sin \theta_i)} \\ &\quad \cdot g_i(\theta_i + \tilde{\theta}, \phi_i + \tilde{\phi}; \mu_i) d\tilde{\theta} d\tilde{\phi}, \end{aligned} \quad (14)$$

Clearly,  $[\mathbf{h}(\mu_i)]_k$  is the real-valued function since  $g_i(\theta_i + \tilde{\theta}, \phi_i + \tilde{\phi}; \mu_i)$  is the even function of  $\tilde{\theta}$  and  $\tilde{\phi}$  because of the symmetry assumption on angular signal distribution. Thus,  $\mathbf{h}(\mu_i)$  is the  $M \times 1$  real-valued vector.

Substitute (12) into (9), and we have:

$$\begin{aligned} [\mathbf{b}_{X_2}(\mu_i)]_k &= e^{j\eta(k-1)\sin \phi_i \cos \theta_i} \iint e^{j\eta(k-1)(\tilde{\phi} \cos \phi_i \cos \theta_i - \tilde{\theta} \sin \phi_i \sin \theta_i)} \\ &\quad \cdot e^{j\eta \sin \phi_i \cos \theta_i} e^{j\eta(\tilde{\phi} \cos \phi_i \cos \theta_i - \tilde{\theta} \sin \phi_i \sin \theta_i)} \\ &\quad \cdot g_i(\theta_i + \tilde{\theta}, \phi_i + \tilde{\phi}; \mu_i) d\tilde{\theta} d\tilde{\phi} \end{aligned} \quad (15)$$

If  $d/\lambda = 1/2$ , for small angular extension, it follows that  $e^{j\eta(\tilde{\phi} \cos \phi_i \cos \theta_i - \tilde{\theta} \sin \phi_i \sin \theta_i)} \approx 1$ . Thus, the above formula can be rewritten as:

$$[\mathbf{b}_{X_2}(\mu_i)]_k \approx e^{j\eta \sin \phi_i \cos \theta_i} e^{j\eta(k-1)\sin \phi_i \cos \theta_i} [\mathbf{h}(\mu_i)]_k \quad (16)$$

From (13) and (16), the following relation holds:

$$\mathbf{b}_{X_2}(\mu_i) \approx e^{j\eta \sin \phi_i \cos \theta_i} \mathbf{b}_{X_1}(\mu_i), \quad (17)$$

and in matrix form:

$$\mathbf{B}_{X_2} \approx \mathbf{B}_{X_1} \Phi_X, \quad (18)$$

where  $\mathbf{B}_{X_1}$  and  $\mathbf{B}_{X_2}$  are the  $(M-1) \times q$  generalized steering matrix, and  $\Phi_X = \text{diag}[e^{j\eta \sin \phi_1 \cos \theta_1}, \dots, e^{j\eta \sin \phi_q \cos \theta_q}]$ . Similarly, by one-order Taylor approximation to the  $k^{\text{th}}$  element of  $\mathbf{a}_Y(\theta, \phi)$  around  $(\theta, \phi) = (\theta_i, \phi_i)$ , we can obtain the following relation

$$\mathbf{b}_{Y_2}(\mu_i) \approx e^{j\eta \sin \phi_i \sin \theta_i} \mathbf{b}_{Y_1}(\mu_i), \quad (19)$$

and in matrix form:

$$\mathbf{B}_{Y_2} \approx \mathbf{B}_{Y_1} \Phi_Y, \quad (20)$$

where  $\mathbf{B}_{Y_1}$  and  $\mathbf{B}_{Y_2}$  are the  $(M-1) \times q$  generalized steering matrix, and

$$\Phi_Y = \text{diag}[e^{j\eta \sin \phi_1 \sin \theta_1}, \dots, e^{j\eta \sin \phi_q \sin \theta_q}]$$

### 3. Parameter Estimation Method

In this section, we will introduce a new parameter estimation method for CD sources by exploiting the approximate rotational invariance relationship in L-shaped array and utilizing the propagator method.

#### 3.1. Estimation of the Central DOAs

Firstly, we consider how estimate the rotational matrices  $\Phi_X$  and  $\Phi_Y$  using propagator. Since it is assumed that CD sources are uncorrelated mutually,  $\mathbf{B}_X$  is of full rank. Thus there are  $q$  rows that are linearly independent in  $\mathbf{B}_X$ , and the other rows are the linear representations of them. Assuming that the first  $q$  rows of  $\mathbf{B}_X$  are linearly independent. Partition  $\mathbf{B}_X$  into:

$$\mathbf{B}_X = \left[ \begin{array}{c} \mathbf{B}_1 \\ \mathbf{B}_2 \end{array} \right] \left\{ \begin{array}{l} q \\ M-q \end{array} \right. \quad (21)$$

Propagator can be defined as the unique linear operator  $\mathbf{P}$  from  $M-q$  dimensional complex space  $C^{M-q}$  to  $q$  dimensional complex space  $C^q$ , and we have

$$\mathbf{P}^H \mathbf{B}_1 = \mathbf{B}_2, \quad (22)$$

In (24),  $\mathbf{P}$  can be calculated by the array  $X$  data matrix  $\mathbf{X} = [\mathbf{x}(1), \mathbf{x}(2), \dots, \mathbf{x}(N)]$ , where  $N$  is the number of snapshots. Partition  $\mathbf{W}$  into

$$\mathbf{X} = \left[ \begin{array}{c} \mathbf{X}_1 \\ \mathbf{X}_2 \end{array} \right] \left\{ \begin{array}{l} q \\ M-q \end{array} \right. \quad (23)$$

where  $\mathbf{X}_1$  is of size  $q \times N$ , and  $\mathbf{X}_2$  is of size  $(M-q) \times N$ .

Using the least squares approach, we can construct the following cost function

$$J(\hat{\mathbf{P}}) = \arg \min_{\hat{\mathbf{P}}} \|\mathbf{X}_2 - \hat{\mathbf{P}}^H \mathbf{X}_1\|^2, \quad (24)$$

where  $\|\cdot\|^2$  denotes Frobenius norm.

Then, the estimation of  $\mathbf{P}$  can be given by:

$$\hat{\mathbf{P}} = (\mathbf{X}_1 \mathbf{X}_1^H)^{-1} \mathbf{X}_1 \mathbf{X}_2^H, \quad (25)$$

Let  $\tilde{\mathbf{P}} = \begin{bmatrix} \mathbf{I}_q \\ \mathbf{P}^H \end{bmatrix}$ , where  $\mathbf{I}_q$  is the  $q \times q$  identity matrix.

According to (24), we have:

$$\tilde{\mathbf{P}} \mathbf{B}_1 = \begin{bmatrix} \mathbf{I}_q \\ \mathbf{P}^H \end{bmatrix} \mathbf{B}_1 = \begin{bmatrix} \mathbf{B}_1 \\ \mathbf{B}_2 \end{bmatrix} = \mathbf{B}_X = \left[ \begin{array}{c} \mathbf{B}_{X_1} \\ \text{the last row} \end{array} \right] = \left[ \begin{array}{c} \text{the first row} \\ \mathbf{B}_{X_2} \end{array} \right] \quad (26)$$

Let  $\tilde{\mathbf{P}}_1$  and  $\tilde{\mathbf{P}}_2$  be the upper and lower  $p \times q$  half matrix of  $\tilde{\mathbf{P}}$ , respectively. From (30), we have:

$$\tilde{\mathbf{P}}_1 \mathbf{B}_1 = \mathbf{B}_{X_1}, \quad (27)$$

$$\tilde{\mathbf{P}}_2 \mathbf{B}_1 = \mathbf{B}_{X_2} \Phi_X, \quad (28)$$

Furthermore, we have:

$$\hat{\Phi}_X = \mathbf{B}_1^{-1} \tilde{\mathbf{P}}_1^+ \tilde{\mathbf{P}}_2 \mathbf{B}_1, \quad (29)$$

where  $\tilde{\mathbf{P}}_1^+ = (\tilde{\mathbf{P}}_1^H \tilde{\mathbf{P}}_1)^{-1} \tilde{\mathbf{P}}_1^H$ ,  $[\cdot]^+$  denotes to solve generalized inverse matrix.

According to similar steps, we can also obtain  $\hat{\Phi}_Y$ .

After obtaining  $\hat{\Phi}_X$  and  $\hat{\Phi}_Y$ , we can complete parameter matching using some parameter matching methods, such as the method in [19].

Suppose  $\gamma_i$  and  $\psi_i$  are, respectively, the primary diagonal corresponding elements of  $\hat{\Phi}_X$  and  $\hat{\Phi}_Y$ , and define  $\alpha_i$  and  $\beta_i$  as:

$$\begin{cases} \alpha_i = \frac{\text{angle}(\gamma_i)}{\eta} = \sin \phi_i \cos \theta_i \\ \beta_i = \frac{\text{angle}(\psi_i)}{\eta} = \sin \phi_i \sin \theta_i \end{cases} \quad (i=1, \dots, q), \quad (30)$$

where  $\text{angle}(\cdot)$  is used to find the phase angle of a complex number.

Using  $\alpha_i$  and  $\beta_i$ , the central DOAs of the  $i$ th source can be estimated by (31).

$$\begin{cases} \hat{\theta}_i = \arctan(\beta_i / \alpha_i) \\ \hat{\phi}_i = \arcsin(\sqrt{\alpha_i^2 + \beta_i^2}) \quad (i=1, \dots, q) \end{cases} \quad (31)$$

### 3.2. Computational Complexity Analysis

In this section, we analyze the computational complexity of the proposed method in comparison with the SOS and QRIP methods. The proposed method doesn't need to perform any peak-finding search, and avoids the estimation and eigendecomposition of high-dimensional sample covariance matrix. Its main computational cost lies

in estimating two  $q$ -diagonal matrices:  $\Phi_X$  and  $\Phi_Y$ . SOS is a classic search-based algorithm, whose calculation is mainly made of three parts: the estimation and eigendecomposition of a  $2M \times 2M$  sample covariance matrix, and twice 1D peak-finding search. QRIP don't require peak-finding search, and its computation mainly embodies in the estimation and eigendecomposition of two sample covariance matrices, whose sizes are, respectively,  $2M \times 2M$  and  $M \times M$ . Table 1 shows the rough computational costs of three methods. It is clear that our approach provide lower computational complexity than other two methods.

Table 1. Comparison of computational complexity.

Method	Number of complex multiplication			
	Estimation of the sample covariance matrix	Eigendecomposition of the sample covariance matrix	Peak-finding search	Total
SOS	$\mathcal{O}(4M^2N)$	$\mathcal{O}(8M^3)$	$\mathcal{O}(2M^6)$	$\mathcal{O}(4M^2N) + \mathcal{O}(8M^3) + \mathcal{O}(2M^6)$
QRIP	$\mathcal{O}(4M^2N) + \mathcal{O}(N^2N)$	$\mathcal{O}(8M^3) + \mathcal{O}(M^3)$	0	$\mathcal{O}(5M^2N) + \mathcal{O}(9M^3)$
Proposed	$\mathcal{O}(2M^2N)$	$\mathcal{O}(2q^3)$	0	$\mathcal{O}(2M^2N) + \mathcal{O}(2q^3)$

### 4. Simulation Results

In this section, some simulation experiments are used to investigate the performance of the proposed method. In our simulations, it is assumed that each of the ULAs  $X$  and  $Y$  contains  $M=10$  sensor elements, and the distance of adjacent sensors in each ULA is  $d = \lambda/2$ . Moreover, all simulation examples are based on 500 Monte Carlo simulations.

In the first example, we compare the proposed method with SOS method for a Gaussian-shaped coherently distributed (GCD) source with  $\mu_i = (-20^\circ, 2^\circ, 40^\circ, 2^\circ)$ . When the number of snapshots is set to  $N=400$ , the root-mean-square errors (RMSEs) of  $\hat{\theta}_i$  and  $\hat{\phi}_i$  estimated by the proposed and SOS methods as well as the Cramer-Rao lower bound (CRB) are illustrated at different SNR in Fig. 2 and Fig. 3. Where, the definition of RMSEs of  $\hat{\theta}_i$  and  $\hat{\phi}_i$  is as follows:

$$\begin{cases} \text{RMSE}_{\theta_i} = \sqrt{E[(\hat{\theta}_i - \theta_i)^2]} \\ \text{RMSE}_{\phi_i} = \sqrt{E[(\hat{\phi}_i - \phi_i)^2]} \end{cases}, \quad (32)$$

We can clearly observe that the DOA estimates not only of the SOS method but also the proposed method attain the CRB as the SNR increase. Further, the performance of the proposed method approaches greatly SOS algorithm.

In the second example, let we consider in Fig. 4 the influence of the number of snapshots on the

performance. Assume that the source is the same as the first example, and SNR=20 dB. It can be observed that our method presents accurate estimation even for a small number of snapshots, and the estimation accuracy of  $\hat{\phi}_i$  is higher than that of  $\hat{\theta}_i$  under the same number of snapshots.

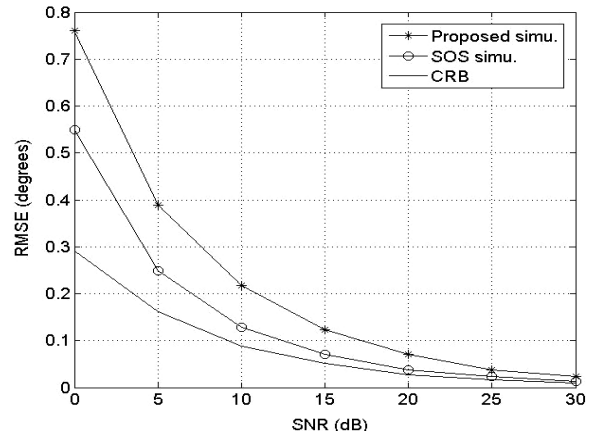


Fig. 2. RMSEs of  $\hat{\theta}_i$  estimated by the proposed and SOS methods versus SNR.

In the third example, the influence of the angular spread on the performance can be deduced from Fig. 5. We have assumed that the source is the same as the first example, SNR=20 dB, and  $N=400$ . It is easily observed that the variations of RMSEs of  $\hat{\theta}_i$  and  $\hat{\phi}_i$  are rather small versus angular extension

when angular spread is smaller than 4 degree, the RMSEs of  $\hat{\theta}_i$  and  $\hat{\phi}_i$  increase significantly versus angular spread when angular spread exceeds 4 degree. Therefore, our method is fitter for the case of small angular spread.

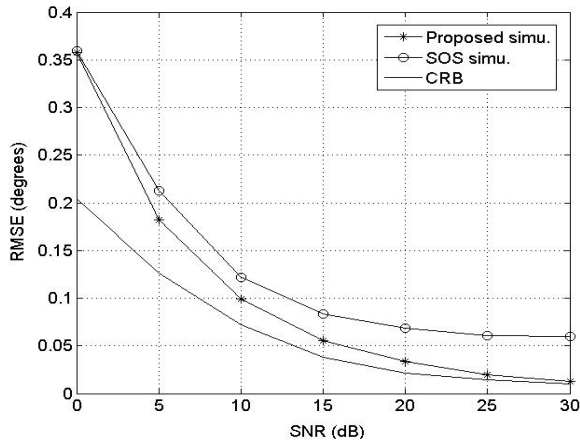


Fig. 3. RMSEs of  $\hat{\phi}_i$  estimated by the proposed and SOS methods versus SNR.

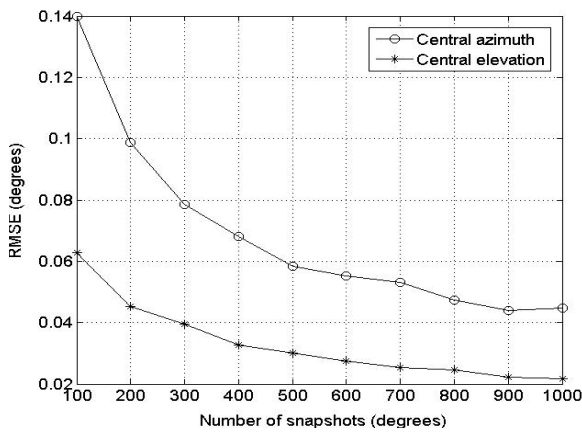


Fig. 4. RMSEs of  $\hat{\theta}_i$  and  $\hat{\phi}_i$  estimated by the proposed method versus snapshots.

In the fourth example, the influence of the central DOA is investigated in Fig. 6. At this time, we assume that a GCD source with  $\sigma_{\theta_i} = \sigma_{\phi_i} = 2^\circ$ , SNR=20dB, and  $N=1000$ . It is easily observed that the RMSE of  $(\hat{\theta}_i, \hat{\phi}_i)$  is smaller than 1 degree when the central azimuth or elevation approach  $90^\circ$ . Where the definition of RMSEs is as follows:

$$RMSE_{(\theta_i, \phi_i)} = \sqrt{E[(\hat{\theta}_i - \theta_i)^2 + (\hat{\phi}_i - \phi_i)^2]} \quad (33)$$

Therefore, the proposed method is applicable to the central azimuth and elevation DOA approaching  $90^\circ$ .

In the fifth example, consider the case of three sources. Two of them are GCD source respectively with  $\mu_1 = (-40^\circ, 1^\circ, 50^\circ, 2^\circ)$  and  $\mu_2 = (30^\circ, 2^\circ, 75^\circ, 2^\circ)$ , other one is uniformly-shaped CD source

with  $\mu_3 = (65^\circ, 2^\circ, 20^\circ, 3^\circ)$ . Assume that the number of snapshots is 1000. Fig. 7 shows the RMSEs of  $(\hat{\theta}_i, \hat{\phi}_i)$  estimated by the proposed method for three sources, respectively, versus the SNR. As it can be seen, the proposed method can estimate accurately multiple CD sources with different angular distributions.

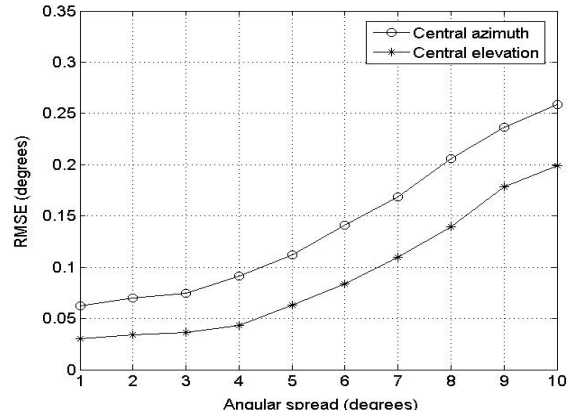


Fig. 5. RMSEs of  $\hat{\theta}_i$  and  $\hat{\phi}_i$  estimated by the proposed method versus angular spread.

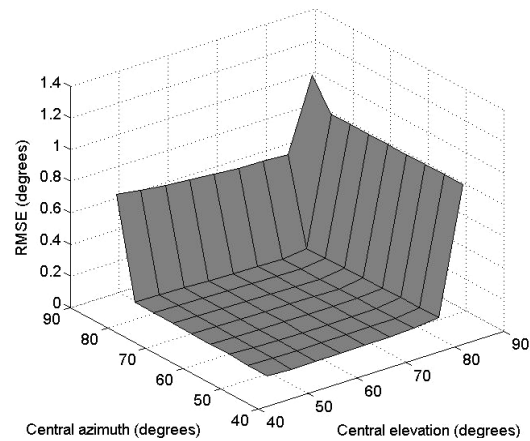


Fig. 6. RMSE of  $(\hat{\theta}_i, \hat{\phi}_i)$  estimated by the proposed method versus central DOA.

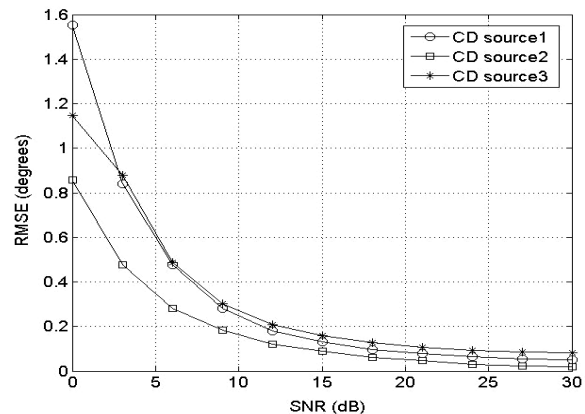


Fig. 7. RMSEs of  $(\hat{\theta}_i, \hat{\phi}_i)$  estimated by the proposed method versus SNR for three CD sources.

## 5. Conclusion

In this paper, a new approach for 2D DOA estimation of CD sources has been presented. The presented method obtains a simplified estimation of the 2D central DOAs by combining propagator technique with the classical estimation methods. Our approach avoids peak-finding search and the eigendecomposition of the high-dimensional sample covariance matrix, and thus requires less computational cost than the conventional methods. Simulation results show that our approach provide a good estimation performance under small angular spread and can estimate the central DOAs of multiple sources with different angular distributions.

## References

- [1]. Valaee, S., Champagne, B. and Kabal, P., Parametric localization of distributed sources, *IEEE Transactions on Signal Processing*, Vol. 43, No. 9, 1995, pp. 2144-2153.
- [2]. Raich, R., Goldberg, J. and Messer, H., Bearing estimation for a distributed source: Modeling, inherent accuracy limitations and algorithms, *IEEE Transactions on Signal Processing*, Vol. 48, No. 2, 2000, pp. 429-441.
- [3]. Lee, Y. U., Lee, S. R., Chang, T., et al., An analysis of DOA estimation method under a dispersive signal model, *ICCSPP*, 1995, pp. 351-354.
- [4]. Tabrikian, J. and Messer, H., Robust localization of scattered sources, *IEEE Workshop on Statistical Signal and Array Processing*, 2000, pp. 453-457.
- [5]. Wu, Q., Wong, K. M. and Meng, Y., DOA Estimation of point and scattered sources: Vec-MUSIC, *IEEE Signal Workshop on SSAP*, 1994, pp. 365-368.
- [6]. Valaee, S., Champagne, B. and Kabal, P., Parametric localization of distributed sources, *IEEE Transactions on Signal Processing*, Vol. 43, No. 9, 1995, pp. 2144-2153.
- [7]. Lee, Y. U., Choi, J., Song, I. and Lee, S. R., Distributed sources modeling and direction-of-arrival estimation techniques, *IEEE Transactions on Signal Processing*, Vol. 4, No. 45, 1997, pp. 960-969.
- [8]. Shahbazpanahi, S., Valaee, S. and Bastani, M. H., Distributed Source Localization Using ESPRIT Algorithm, *IEEE Transactions on Signal Processing*, Vol. 49, No. 10, 2001, pp. 2169-2178.
- [9]. Wan, Q. and Peng, Y. N., Low-complexity estimator for four-dimensional parameters under a reparameterised distributed source model, *IEE Proc. Radar, Sonar Navigation*, Vol. 148, No. 6, 2001, pp. 313-317.
- [10]. Wan, Q. and Yang, W. L., Low-complexity estimator for two-dimensional DOA under a distributed source model, *CIE Radar*, 2001, pp. 814-818.
- [11]. Wan, Q. and Yang, W. L., Approach for direction of arrival estimation with sensor gain uncertainties, *Acta Electr Sin*, Vol. 29, No. 6, 2001, pp. 730-732.
- [12]. Wan, Q. and Yang, W. L., Approach for 1-dimensional direction of arrival estimation of coherently distributed sources in noise, *Signal Process China*, Vol. 27, No. 2, 2000, pp. 115-119.
- [13]. Zoubir, A. Wang, Y. D. and Charge, P., New adaptive beamformers for estimation of spatially distributed sources, in *Proceedings of the IEEE Antennas and Propagation Society International Symposium*, 2004, pp. 2643-2646.
- [14]. Guo, X. S., Wan, Q., Wu, B. and Yang, W. L., Parameters localization of coherently distributed sources based on sparse signal representation, *IEE Proc. Radar, Sonar Navigation*, Vol. 1, No. 4, 2007, pp. 261-265.
- [15]. Lee, S. R., Song, I., Chang, T., et al., Distributed source location estimation using a circular array, *ISSPA*, 1996, pp. 341-344.
- [16]. Lee, S. R., Song, I., Lee, Y. U. and Kim, H. G., Estimation of distributed elevation and azimuth angles using linear arrays, *MILCOM*, 1996, pp. 868-872.
- [17]. Lee, J., Song, I., Kwon, H. and Lee, S. R., Low-complexity estimation of 2D DOA for coherently distributed sources, *Signal Processing*, Vol. 83, 2003, pp. 1789-1802.
- [18]. Guo, X. S., Wan, Q., Yang, W. L., et al., Low-complexity 2D coherently distributed sources decoupled DOAs estimation method, *Sci China Ser F-Inf. Sci*, Vol. 52, No. 5, 2009, pp. 835-842.
- [19]. Zheng, Z., Li, G. J. and Teng, Y. L., Low-complexity 2D DOA estimator for multiple coherently distributed sources, *COMPEL*, Vol. 31, No. 2, 2012, pp. 443-459.
- [20]. Marcos, S., Marsal, A. and Benidir, M., The propagator method for source bearing estimation, *Signal Processing*, Vol. 42, No. 2, 1995, pp. 121-138.